Generation of X-Rays by Laser Accelerated Electrons

Vojtěch Horný

26th September 2018

Czech Technical University in Prague
Faculty of Nuclear Sciences and Physical Engineering
Department of Physical Electronics

e-mail address: horny@ipp.cas.cz

List of Contents

1. Motivation: X-rays
2. Laser wakefield acceleration
3. Electron bunch injection into the wakefield
4. X-rays from laser accelerated electrons
5. Temporal profile of X-ray betatron radiation
6. Conclusions

Motivation

X-rays and their sources

- X-ray radiation is a part of electromagnetic spectrum with $E_{ph} \gtrsim$ **250 eV**.
- **Wilhelm Conrad Röntgen** (discovery in 1895, first Nobel prize in 1901).
- X-rays are exploited in fundamental and applied research, medical and industrial applications, public security, . . .
- They are currently delivered by
  - radioactive sources
  - X-ray tubes
  - devices based on electron accelerators such as **synchrotron**.

European XFEL (X-Ray Free Electron Laser)

- 2.1 km long linear electron accelerator + 210 m undulator.
- coherent X-rays with photon energy of 0.25–25 keV and pulse energy of 0.5–10 mJ.
- large investment and operation costs

X-Rays from Laser Accelerated Electrons

Benefits over conventional sources

1. Shortening of the X-ray pulse duration
   - current sources sub-picosecond (sliced synchrotron beamlines)
   - typical vibration period in atoms in order of tens of fs
   - fundamental physical processes such as electron transfer, lattice vibrations, phase transitions, chemical reactions or spin dynamics could be observed with shorter X-ray pulses.
2. Reduction of X-ray source size
   - enhancement of absorption radiography resolution
   - X-ray phase contrast imaging
3. Financial availability
   - 100TW laser system as small as one (large) optical table

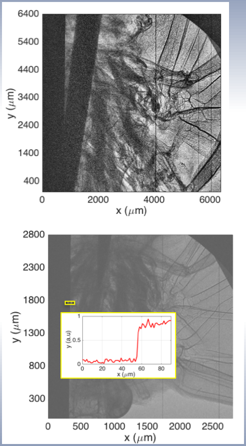

Dry moth facing betatron radiation with $E_c = 3.3$ keV [U. Chaulagain, SPIE Prague 2017].

Laser wakefield acceleration

- Ultrashort (tens of fs) ultraintense ($\gtrsim 10^{19}$ W/cm^2) laser pulse interacts with the underdense plasma ($n_e \approx 10^{18-19}$ cm^{-3}).
- Strong non-linear ponderomotive force ($\sim \nabla I$) expels light electrons out of high intensity region.
- Strong electron plasma wave (wakefield, $\sim$ 100 GV/m) arises behind the laser pulse.
- Electrons can be accelerated at this plasma wave similarly like a surfer at the wake wave.

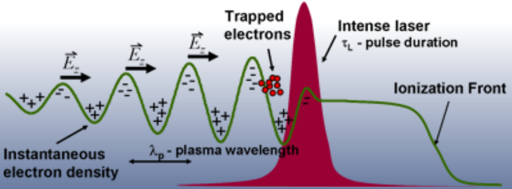

Courtesy: Michigan Engieering Center for Ultrafast Optical Science

Interaction laser vs. free electron in vacuum

Pulse parameters are $\lambda_L = 0.8$ µm, $w_0 = 9.5$ µm, $\tau = 25$ fs, $a_0 = 4$.

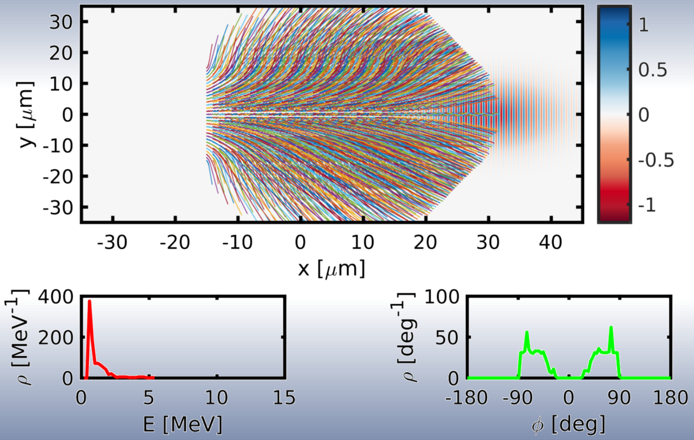

Nonlinear plasma wave: 1D model

Poisson's equation[1]

$$\frac{1}{k_p^2}\frac{\mathrm{d}^2\phi}{\mathrm{d}\,\xi^2} = \gamma_p^2\left\{\beta_p\left[1-\frac{1+a^2(\xi)}{\gamma_p^2(1+\phi(\xi))^2}\right]^{-1/2}-1\right\},$$

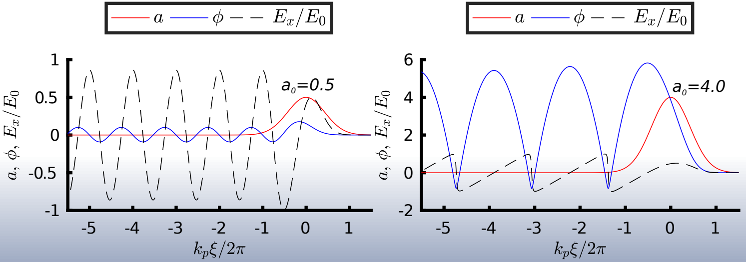

Pulse duration: 25 fs, electron density 5×10^{18} W/cm^2.

[1]Assumptions: zero electron temperature and ions at rest.

Electron motion in nonlinear 1D plasma wave

$H(\xi, u_x) = \sqrt{1 + a^2(\xi) + u_x^2} - \phi(\xi) - \beta_p u_x$ is constant.

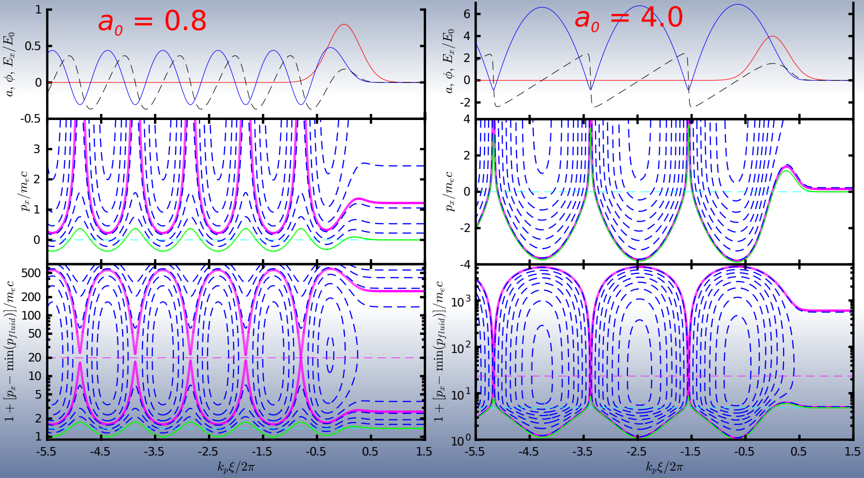

Electron injection into accelerating phase

- The main challenge nowadays: production of electron bunches with **well defined parameters** in a **stable** way.
- **Self-injection** is a simple, but unstable mechanism to inject electron into plasma wave.
- Possible solution: to separate injection and acceleration processes.

Several injection mechanisms considered

- external injection,
- ionisation injection,
- injection by density ramp,
- optical injection.

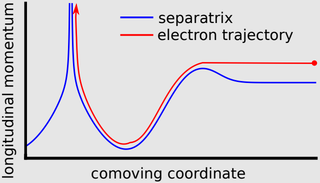

Motivation

Features of generated X-rays are determined by properties of accelerated electron bunch.

Electron injection into accelerating phase

- The main challenge nowadays: production of electron bunches with **well defined parameters** in a **stable** way.
- **Self-injection** is a simple, but unstable mechanism to inject electron into plasma wave.
- Possible solution: to separate injection and acceleration processes.

Several injection mechanisms considered

- external injection,
- ionisation injection,
- injection by density ramp,
- optical injection.

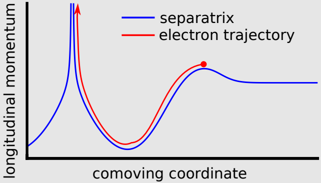

Motivation

Features of generated X-rays are determined by properties of accelerated electron bunch.

Electron injection into accelerating phase

- The main challenge nowadays: production of electron bunches with **well defined parameters** in a **stable** way.
- **Self-injection** is a simple, but unstable mechanism to inject electron into plasma wave.
- Possible solution: to separate injection and acceleration processes.

Several injection mechanisms considered

- external injection,
- ionisation injection,
- injection by density ramp,
- optical injection.

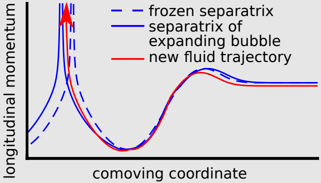

Motivation

Features of generated X-rays are determined by properties of accelerated electron bunch.

Electron injection into accelerating phase

- The main challenge nowadays: production of electron bunches with **well defined parameters** in a **stable** way.
- **Self-injection** is a simple, but unstable mechanism to inject electron into plasma wave.
- Possible solution: to separate injection and acceleration processes.

Several injection mechanisms considered

- external injection,
- ionisation injection,
- injection by density ramp,
- optical injection.

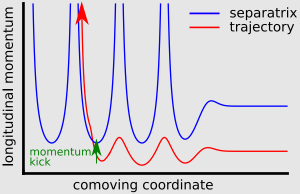

Motivation

Features of generated X-rays are determined by properties of accelerated electron bunch.

Optical injection into ion cavity

Umstadter, PRL 1996 | **Wang, APL 2008** | **Esarey, PRL, 1997 Lehe, PRL, 2013**

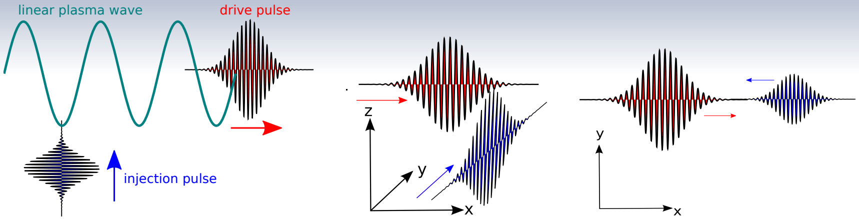

- Originally, optical injection considered for linear regime ($a_0 \lesssim 2$) to avoid self-injection.
- Lehe suggested *cold* optical injection by counter-propagating pulses with strong drive pulse ($a_0 \gtrsim 4$) and weak injection pulse ($a_0 \sim 0.2$).
- We propose the crossing pulses schemes with the strong drive pulse and weak injection pulse [Horný et al., PoP, 2017].

Spectra of accelerated electrons

Typical case of bubble regime

- drive pulse intensity $a_{0,DP} = 4$ ($I_{DP} = 3.42 \times 10^{19}$ W/cm^2)
- waist size $w_0 = 9.5$ µm
- laser wavelength $\lambda_L = 0.8$ µm
- electron density $n_0 = 5 \times 10^{18}$ cm^{-3}
- laser pulse duration $\tau = 25$ fs

Various ratios of $I_{IP}/I_{DP} \in [0.001, 1]$

- optimum found for $I_{IP}/I_{DP} \approx 0.01$.
- Spectrum is divided into two parts ⇒ low energy part can be easily filtered ⇒ very **narrow spectrum** being obtained
- t =8 ps: $E_{el} = (634 \pm 24)$ MeV

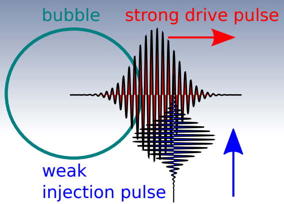

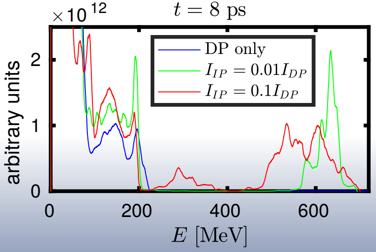

Acceleration process

Evolution of the electron density

drive pulse only

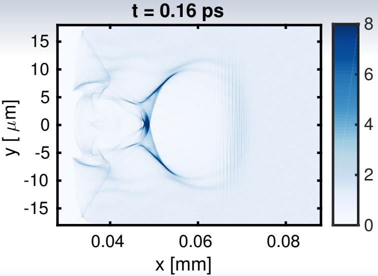

$I_{IP} = 0.01 I_{DP}$.

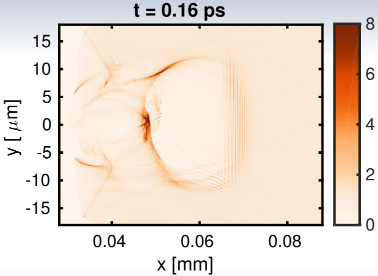

Acceleration process

Evolution of the electron density

drive pulse only

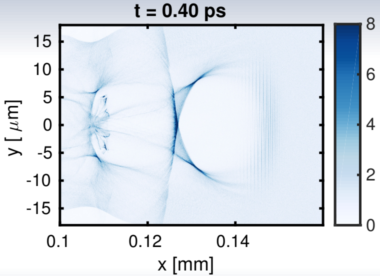

$I_{IP} = 0.01 I_{DP}$.

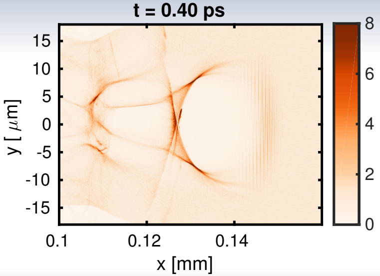

Acceleration process

Evolution of the electron density

drive pulse only

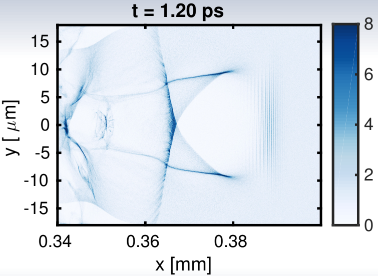

$I_{IP} = 0.01 I_{DP}$.

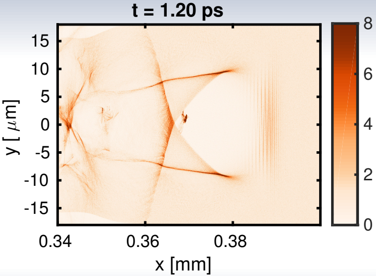

Acceleration process

Evolution of the electron density

drive pulse only

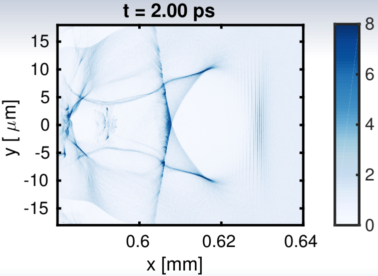

$I_{IP} = 0.01 I_{DP}$.

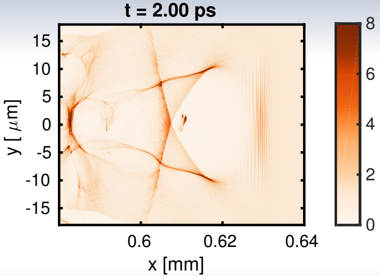

Acceleration process

Evolution of the electron density

drive pulse only

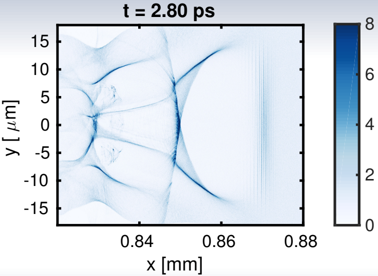

$I_{IP} = 0.01 I_{DP}$.

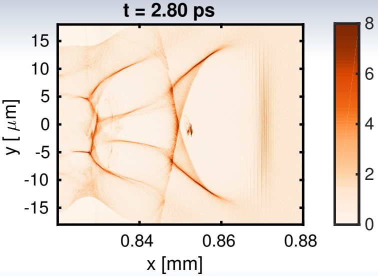

Acceleration process

Evolution of the electron density

drive pulse only

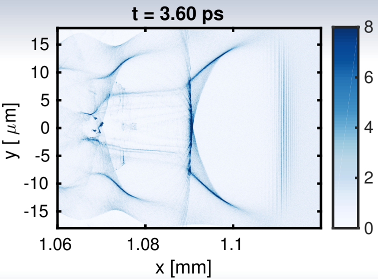

$I_{IP} = 0.01 I_{DP}.$

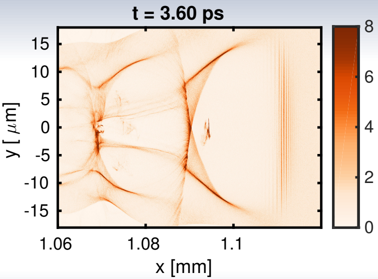

Acceleration process

Evolution of the electron density

drive pulse only

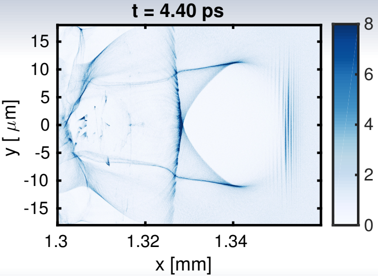

$I_{IP} = 0.01 I_{DP}$.

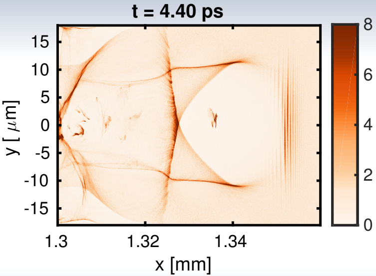

Acceleration process

Evolution of the electron density

drive pulse only

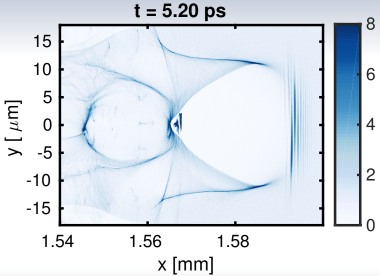

$I_{IP} = 0.01 I_{DP}$.

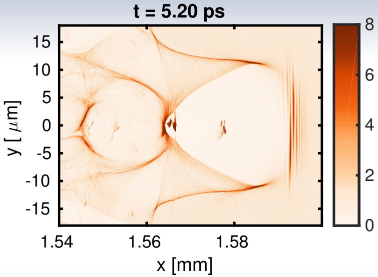

Acceleration process

Evolution of the electron density

drive pulse only | $I_{IP} = 0.01 I_{DP}$.

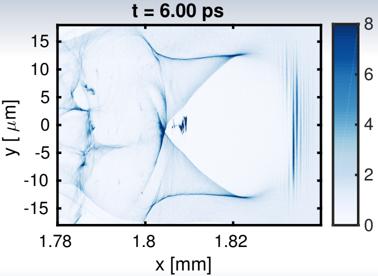

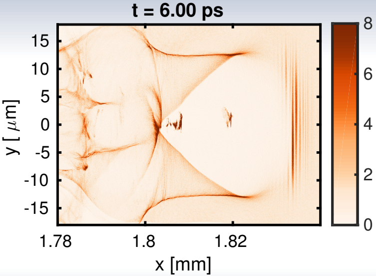

Observation

Injection pulse does not disturb bubble dynamics and self-injection when it is very weak in comparison with main beam.

Three injection mechanisms

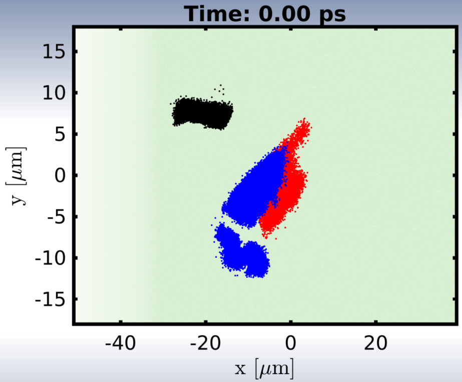

crossing beatwave injection	≈ 70 % of trapped electrons
injection by laser field pre-acceleration	≈ 20 % of trapped electrons
induced self-injection	≈ 10 % of trapped electrons

Three injection mechanisms

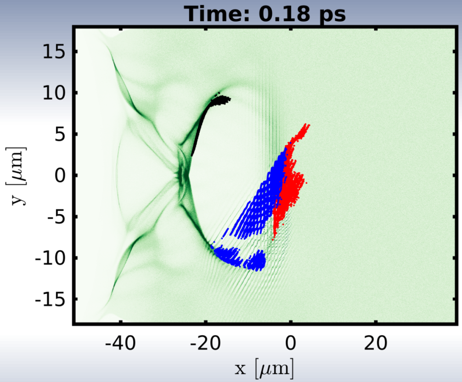

crossing beatwave injection	≈ 70 % of trapped electrons
injection by laser field pre-acceleration	≈ 20 % of trapped electrons
induced self-injection	≈ 10 % of trapped electrons

Three injection mechanisms

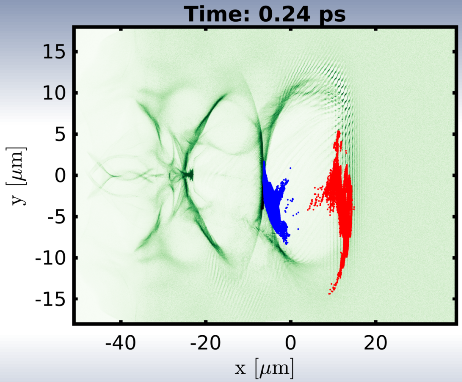

crossing beatwave injection	$\approx$ 70 % of trapped electrons
injection by laser field pre-acceleration	$\approx$ 20 % of trapped electrons
induced self-injection	$\approx$ 10 % of trapped electrons

Three injection mechanisms

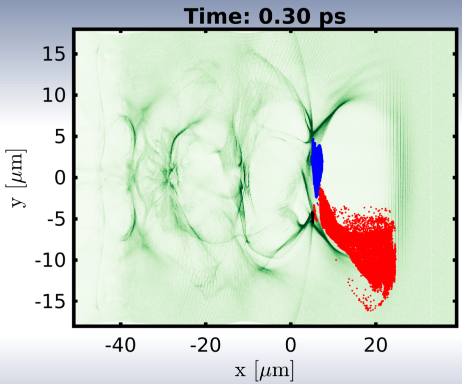

crossing beatwave injection ≈ 70 % of trapped electrons
injection by laser field pre-acceleration ≈ 20 % of trapped electrons
induced self-injection ≈ 10 % of trapped electrons

Three injection mechanisms

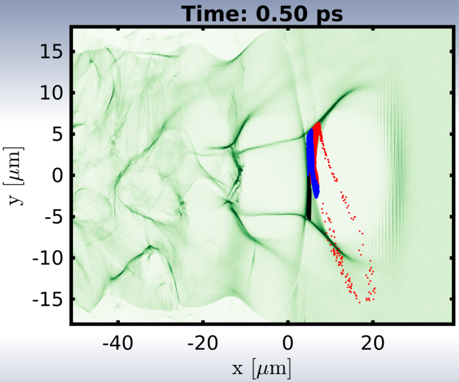

crossing beatwave injection ≈ 70 % of trapped electrons
injection by laser field pre-acceleration ≈ 20 % of trapped electrons
induced self-injection ≈ 10 % of trapped electrons

Three injection mechanisms

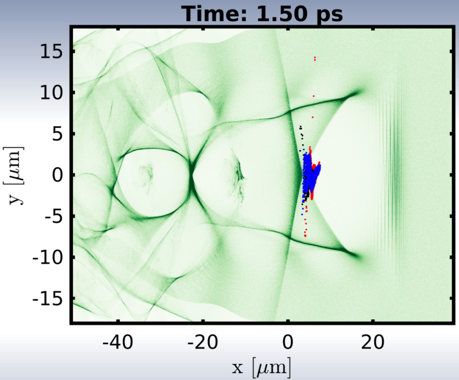

crossing beatwave injection	≈ 70 % of trapped electrons
injection by laser field pre-acceleration	≈ 20 % of trapped electrons
induced self-injection	≈ 10 % of trapped electrons

Three injection mechanisms

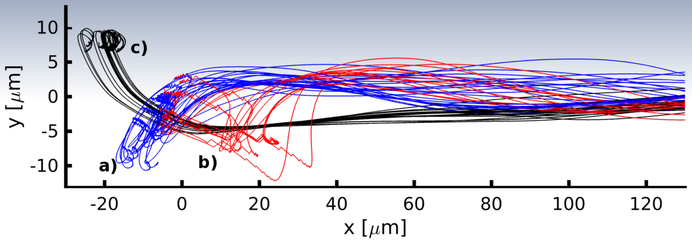

crossing beatwave injection	≈ 70 % of trapped electrons
injection by laser field pre-acceleration	≈ 20 % of trapped electrons
induced self-injection	≈ 10 % of trapped electrons

Three injection mechanisms

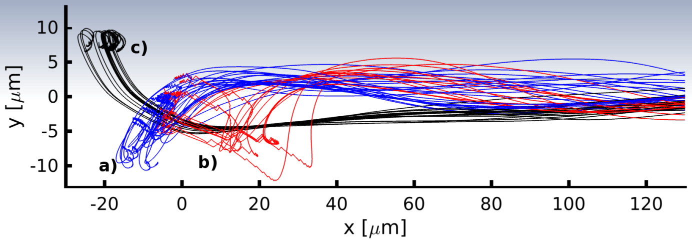

crossing beatwave injection	$\approx$ 70 % of trapped electrons
injection by laser field pre-acceleration	$\approx$ 20 % of trapped electrons
induced self-injection	$\approx$ 10 % of trapped electrons

Consequence

Relatively high emittance of 2.88 $\pi \cdot$mm$\cdot$mrad.

Electrons in the field of crossed pulses

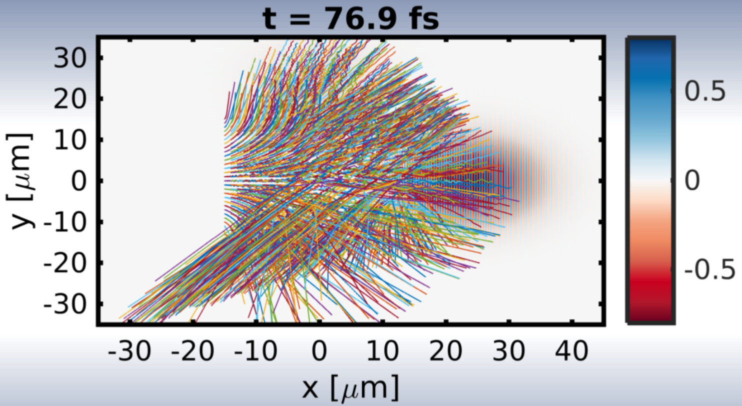

Test particle simulations for $a_{0,DP} = 4$, $a_{0,IP} = 0.2$. 961 electrons.
Colour bar in the unit of B_z peak value of the drive pulse.

Electrons in the field of the bubble

$$E_x = \frac{m_e \omega_p^2}{2|e|}\xi, \qquad E_y = \frac{m_e \omega_p^2}{4|e|}y, \qquad B_z = -\frac{m_e \omega_p^2}{4|e|c}y$$

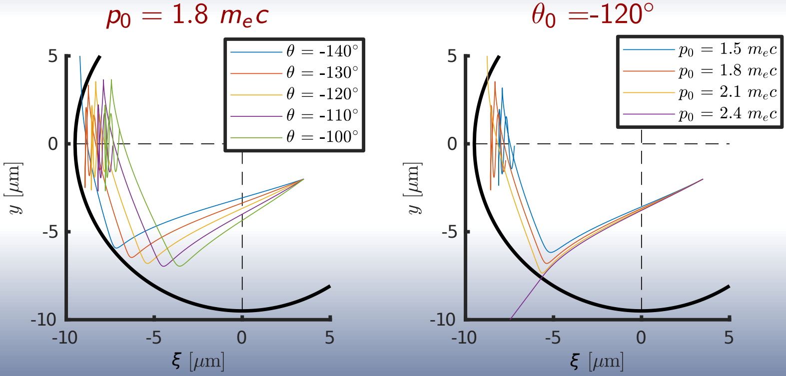

Electrons initially located at point **[3.5 μm, -2 μm]**.

Other observations

1. Electron beams characteristics only weakly depends on short delay between pulses. Injected charge is the greatest if pulses meet *in time*.

[1] Golovin, Grigory, et al. "Electron Trapping from Interactions between Laser-Driven Relativistic Plasma Waves." Physical Review Letters 121.10 (2018): 104801.

Other observations

1. Electron beams characteristics only weakly depends on short delay between pulses. Injected charge is the greatest if pulses meet *in time*.
2. Same waist size of drive and injection pulses seems to be optimum choice.

[1] Golovin, Grigory, et al. "Electron Trapping from Interactions between Laser-Driven Relativistic Plasma Waves." Physical Review Letters 121.10 (2018): 104801.

Other observations

1. Electron beams characteristics only weakly depends on short delay between pulses. Injected charge is the greatest if pulses meet *in time*.
2. Same waist size of drive and injection pulses seems to be optimum choice.
3. Mutual perpendicular polarizations of both pulses seems to provide rather more mononergetic bunches than in case of parallel polarizations for the cost of lower charge.

[1] Golovin, Grigory, et al. "Electron Trapping from Interactions between Laser-Driven Relativistic Plasma Waves." Physical Review Letters 121.10 (2018): 104801.

Other observations

1. Electron beams characteristics only weakly depends on short delay between pulses. Injected charge is the greatest if pulses meet *in time*.
2. Same waist size of drive and injection pulses seems to be optimum choice.
3. Mutual perpendicular polarizations of both pulses seems to provide rather more mononergetic bunches than in case of parallel polarizations for the cost of lower charge.
4. Discussed regime works well in electron densities $2 - 10 \times 10^{18}$ W/cm^2.

[1] Golovin, Grigory, et al. "Electron Trapping from Interactions between Laser-Driven Relativistic Plasma Waves." Physical Review Letters 121.10 (2018): 104801.

Other observations

1. Electron beams characteristics only weakly depends on short delay between pulses. Injected charge is the greatest if pulses meet *in time*.
2. Same waist size of drive and injection pulses seems to be optimum choice.
3. Mutual perpendicular polarizations of both pulses seems to provide rather more mononergetic bunches than in case of parallel polarizations for the cost of lower charge.
4. Discussed regime works well in electron densities $2 - 10 \times 10^{18}$ W/cm^2.

[1] Golovin, Grigory, et al. "Electron Trapping from Interactions between Laser-Driven Relativistic Plasma Waves." Physical Review Letters 121.10 (2018): 104801.

Other observations

1. Electron beams characteristics only weakly depends on short delay between pulses. Injected charge is the greatest if pulses meet *in time*.
2. Same waist size of drive and injection pulses seems to be optimum choice.
3. Mutual perpendicular polarizations of both pulses seems to provide rather more mononergetic bunches than in case of parallel polarizations for the cost of lower charge.
4. Discussed regime works well in electron densities $2 - 10 \times 10^{18}$ W/cm^2.

Recent news

An experiment[1] with crossed pulses $a_0 = 1.4$, $a_1 = 8.9$, $n_e \lesssim 1.3 \times 10^{19}$ cm^{-3}, $\varphi = 155^\circ$ proved the **technical feasibility** of the configuration and **confirmed beatwave injection** mechanism.

[1] Golovin, Grigory, et al. "Electron Trapping from Interactions between Laser-Driven Relativistic Plasma Waves." Physical Review Letters 121.10 (2018): 104801.

Comparison: counter-propagating pulse

Presented injection scheme

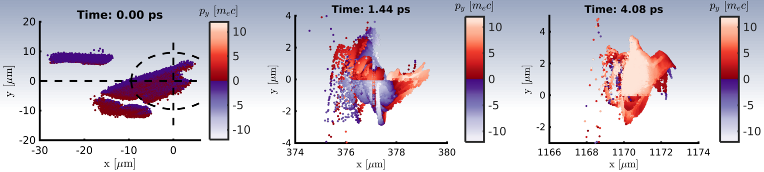

Injection by the counter-propagating pulse

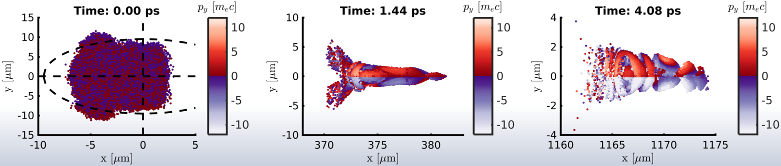

Comparison: counter-propagating pulse

Presented injection scheme

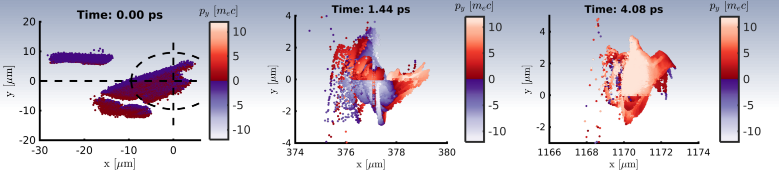

Injection by the counter-propagating pulse

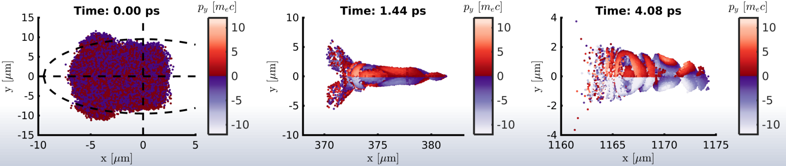

Proposed scheme leads to the **more compact** and **shorter** electron bunch than the one of the injection by the counter-propagating pulses at the same laser and plasma conditions.

Comparison: counter-propagating pulse

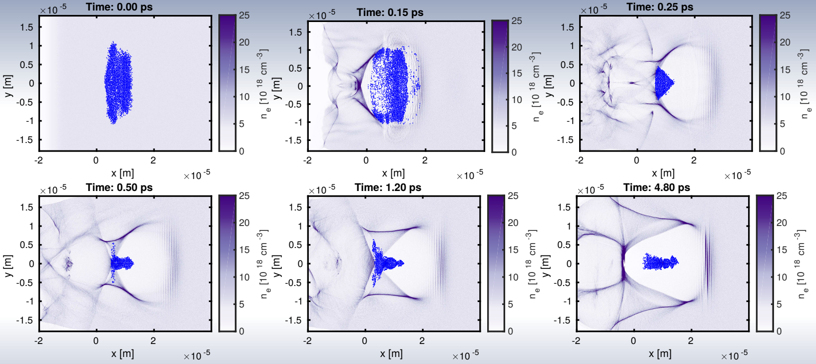

- For the same laser and plasma parameters, the length of the electron bunch is much larger.
- Injected electrons are initially located in the whole region of pulses collision.

Injection by a preceding pulse

Bubble radii [Benedetti, PoP, 2013]

$$R_{\|,0,1} = k_p^{-1}(2.9 + 0.305 a_{0,1})$$

Collection volume [Benedetti, PoP, 2013]

$$r_0 = k_p^{-1}(-2.0 + 1.4 a_0 - 0.05 a_0^2)$$

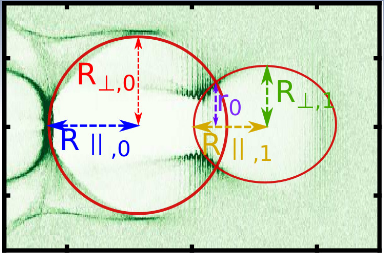

Optimal delay between pulses for an elliptical bubble.

$$\Delta t = \frac{1}{c}\left(R_{\|,0}\sqrt{1-\frac{r_0^2}{R_{\perp,0}^2}} + R_{\|,1}\sqrt{1-\frac{r_0^2}{R_{\perp,1}^2}}\right) + \frac{\tau}{2}$$

Injection by a preceding pulse

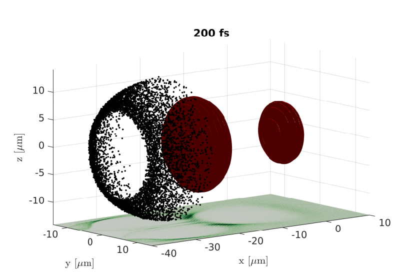

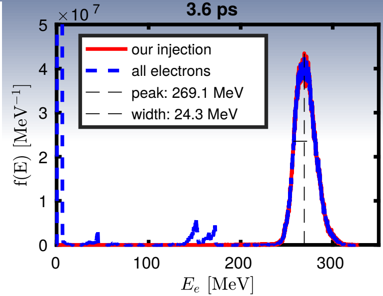

Parameters and results

$n_e = 3 \times 10^{18}$ cm^{-3}, $a_0 = 4$, $a_1 = 2.5$, $\tau_{0,1} = 25$ fs, $\Delta\tau = 65$ fs, $w_{0,1} = 9.5$ μm

$Q = 188$ pC, $\varepsilon_r = 1.63$ $\pi\cdot$mm$\cdot$mrad, $D = 1.8$ μm

Injection by a preceding pulse

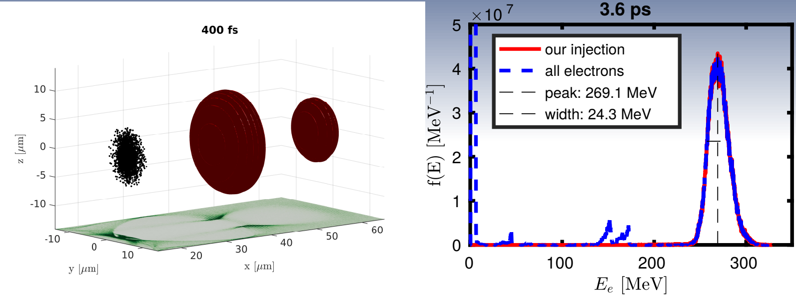

Parameters and results

$n_e = 3 \times 10^{18}$ cm^{-3}, $a_0 = 4$, $a_1 = 2.5$, $\tau_{0,1} = 25$ fs, $\Delta\tau = 65$ fs, $w_{0,1} = 9.5$ μm

$Q = 188$ pC, $\varepsilon_r = 1.63$ $\pi\cdot$mm$\cdot$mrad, $D = 1.8$ μm

X-Rays from laser accelerated electrons

Betatron radiation

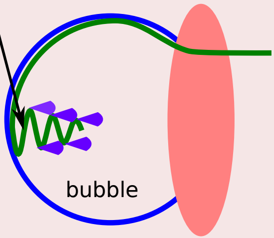

Thomson backscattering

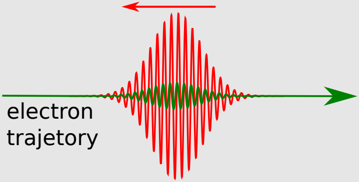

Principle of radiation emission

Transverse oscillation of accelerated electrons!

Radiation by a moving charge

Retarded time

$$t' = t - \frac{|\mathbf{R}|}{c}$$

$$\frac{\mathrm{d}t}{\mathrm{d}t'} = 1 - \mathbf{n}(t')\beta(t')$$

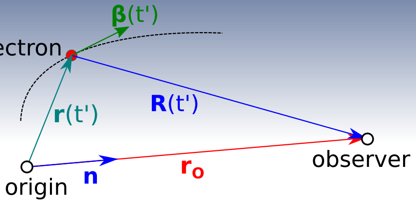

Electric field at observer's position

$$\mathbf{E}(\mathbf{r}_{\mathrm{O}}, t) = \frac{e}{4\pi\varepsilon_0} \left\{ \underbrace{\frac{(1-\beta^2)(\mathbf{n}-\beta)}{R^2(1-\mathbf{n}\cdot\beta)^3}}_{\text{velocity field}} + \underbrace{\frac{\mathbf{n}\times[(\mathbf{n}-\beta)\times\dot{\beta}]}{cR(1-\beta\cdot\mathbf{n})^3}}_{\text{acceleration field}} \right\}_{ret}$$

Radiation by a moving charge

Retarded time

$$t' = t - \frac{|\mathbf{R}|}{c}$$

$$\frac{\mathrm{d}t}{\mathrm{d}t'} = 1 - \mathbf{n}(t')\beta(t')$$

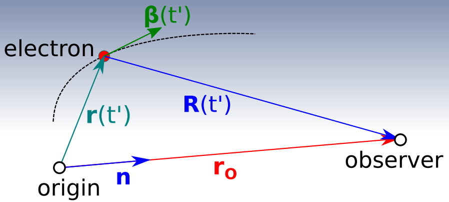

Electric field at observer's position

$$\mathbf{E}(\mathbf{r}, t) = \frac{e}{4\pi\varepsilon_0} \left\{ \underbrace{\cancel{\frac{(1-\beta^2)(\mathbf{n}-\beta)}{R^2(1-\mathbf{n}\cdot\beta)^3}}}_{\text{velocity field}} + \underbrace{\frac{\mathbf{n}\times[(\mathbf{n}-\beta)\times\dot{\beta}]}{cR(1-\beta\cdot\mathbf{n})^3}}_{\text{acceleration field}} \right\}_{ret}$$

Betatron radiation

Chosen approach

Presented in V. Horný *et al.*, Phys. Plas., **24**, 063107, 2017.

$$\frac{\mathrm{d}\mathcal{E}}{\mathrm{d}\Omega} = c\varepsilon_0 \int_{-\infty}^{+\infty} |R(t)\mathbf{E}(t)|^2 \,\mathrm{d}t = \frac{c\varepsilon_0}{\pi} \int_{0}^{+\infty} |\mathfrak{F}[R(t)\mathbf{E}(t)](\omega)|^2 \,\mathrm{d}\omega$$

$$\frac{\mathrm{d}^2 I}{\mathrm{d}\omega \mathrm{d}\Omega} = \frac{c\varepsilon_0}{\pi} |\mathfrak{F}[R(t)\mathbf{E}(t)](\omega)|^2$$

Alternative integral approach

Presented e.g. in A. Thomas, PRSTAB, **13**, 020702, 2010 or Chen *et al.*,PRSTAB **16**, 030701, 2013.

$$\frac{\mathrm{d}^2 I}{\mathrm{d}\omega \mathrm{d}\Omega} = \frac{q^2}{16\pi^3 \varepsilon_0 c} \times \left| \int_{-\infty}^{\infty} \mathrm{e}^{i\omega\left[t' - \frac{\mathbf{n}\cdot\mathbf{R}(t')}{c}\right]} \times \frac{\mathbf{n} \times [(\mathbf{n} - \boldsymbol{\beta}) \times \dot{\boldsymbol{\beta}}]}{(1 - \boldsymbol{\beta}\cdot\mathbf{n})^2} \mathrm{d}t' \right|^2$$

Shannon-Niquist-Kotelnikov-Whittaker theorem

The core of the method is to perform Fourier transform of $R(t)\mathbf{E}(t)$:

$$\frac{\mathrm{d}^2 I}{\mathrm{d}\omega \mathrm{d}\Omega} = \frac{c\varepsilon_0}{\pi} \left|\mathfrak{F}[R(t)\mathbf{E}(t)](\omega)\right|^2 .$$

Sampling frequency must be at least **twice** as high as the highest frequency component of sampled signal!

Signal must be properly sampled to capture X-rays!

E_{ph}	$\nu_{ph} = E_{ph}/h$	$\nu_{sampling}$	Δt
15 keV	3.64×10^{18} Hz	7.28×10^{18} Hz	0.137 as
1 MeV	2.42×10^{20} Hz	4.84×10^{20} Hz	2.06 zs

Typical step in PIC simulations is 0.01-0.1 fs + signal is not sampled equidistantly $\Rightarrow$ **re-interpolation necessary!**

Undulator and wiggler regime

Distinguished by K parameter

$$K = \Psi\gamma = r_\beta k_p \sqrt{\frac{\gamma}{2}}$$

In practical units, K parameter can be expressed as

$$K = 1.33 \times 10^{-10} \sqrt{\gamma n_e \ [\mathrm{cm}^{-3}]} r_\beta \ [\mu\mathrm{m}].$$

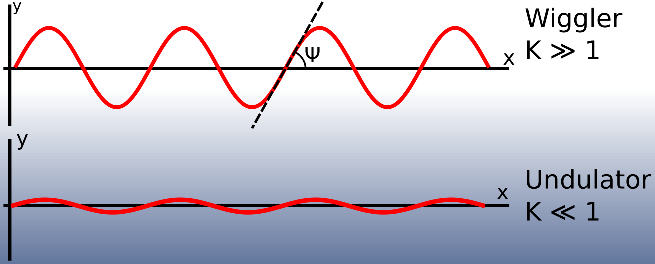

Radiation in undulator and wiggler case

Undulator regime: Fourier series comprises only of single harmonic.

$$K = 0.066$$

Radiation emitted along longitudinal axis

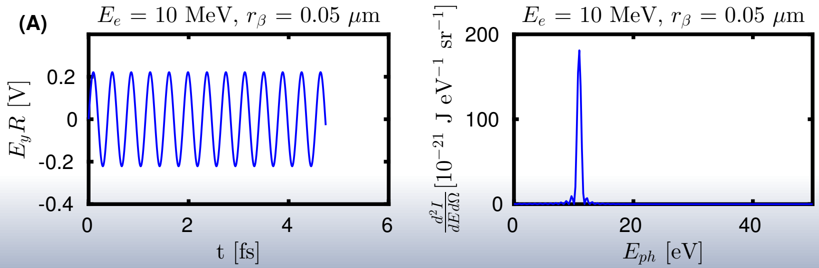

The electron trajectory was calculated using the model presented e.g. in [Corde et al., RMP, 2013] for the ambient electron density $n_e = 5 \times 10^{18}$ cm^{-3}.
Radiated intensity in agreement with the theoretical model [Esarey et al., PRE, 2002].

Radiation in undulator and wiggler case

Mixed regime: Fourier series comprises of several odd harmonics. Even ones vanishes.

$$K = 1.0$$

Radiation emitted along longitudinal axis

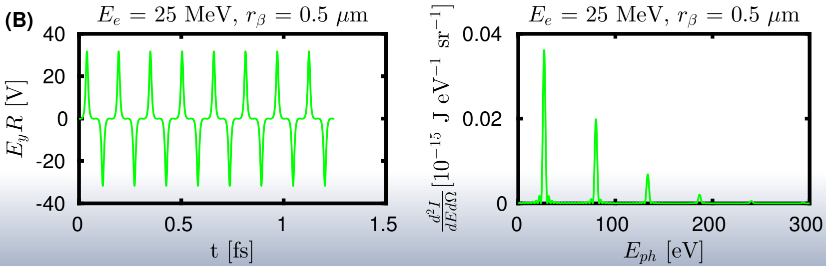

The electron trajectory was calculated using the model presented e.g. in [Corde et al., RMP, 2013] for the ambient electron density $n_e = 5 \times 10^{18}$ cm^{-3}.
Radiated intensity in agreement with the theoretical model [Esarey et al., PRE, 2002].

Radiation in undulator and wiggler case

Mixed regime: Fourier series comprises of several odd harmonics. Even ones vanishes.

$$K = 3.15$$

Radiation emitted along longitudinal axis

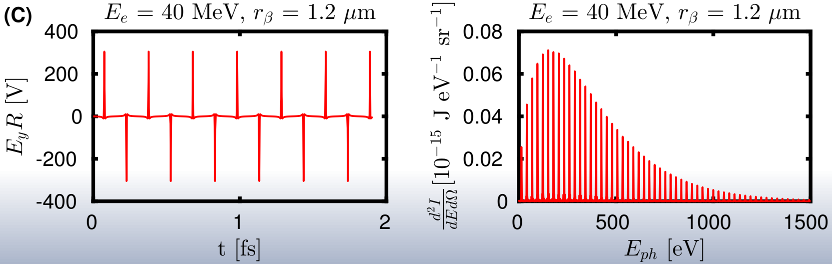

The electron trajectory was calculated using the model presented e.g. in [Corde et al., RMP, 2013] for the ambient electron density $n_e = 5 \times 10^{18}$ cm^{-3}.
Radiated intensity in agreement with the theoretical model [Esarey et al., PRE, 2002].

Radiation in undulator and wiggler case

Wiggler regime: many very closely spaced harmonics can be considered as a continuous synchrotron spectrum.

$$K = 5.46$$

Radiation emitted along longitudinal axis

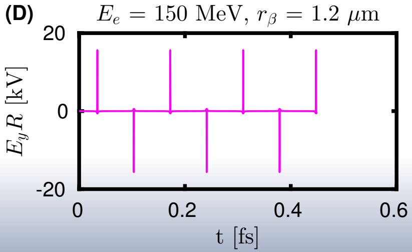

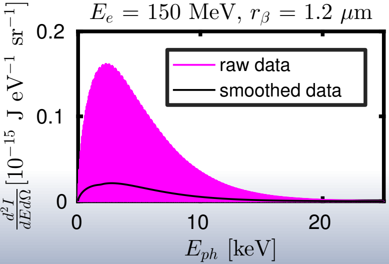

The electron trajectory was calculated using the model presented e.g. in [Corde et al., RMP, 2013] for the ambient electron density $n_e = 5 \times 10^{18}$ cm^{-3}.
Radiated intensity in agreement with the theoretical model [Esarey et al., PRE, 2002].

Simplification for wiggler case

Signal can be understood as a sum of contributions by single peaks

$$\mathbf{E}(t)R(t) = \mathbf{u}(t) = \sum_{j=1}^{N_p} \mathbf{u}_j(t),$$

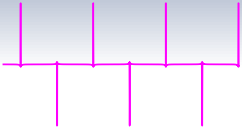

$$\mathbf{u}_j(t) = \begin{cases} \mathbf{E}(t)R(t) & |t - t_j| < \Delta t \\ 0 & \text{otherwise.} \end{cases}$$

Radiated energy per solid angle is then

$$\begin{aligned} \frac{\mathrm{d}\mathcal{E}}{\mathrm{d}\Omega} &= c\varepsilon_0 \int_{-\infty}^{+\infty} \left| \sum_{j=1}^{N_p} \mathbf{u}_j(t) \right|^2 \mathrm{d}t \overset{!}{=} c\varepsilon_0 \int_{-\infty}^{+\infty} \sum_{j=1}^{N_p} |\mathbf{u}_j(t)|^2 \, \mathrm{d}t \\ &= c\varepsilon_0 \sum_{j=1}^{N_p} \int_{-\infty}^{+\infty} |\mathbf{u}_j(t)|^2 \, \mathrm{d}t = \frac{c\varepsilon_0}{\pi} \sum_{j=1}^{N_p} \int_0^{+\infty} |\mathfrak{F}[\mathbf{u}_j(t)](\omega)|^2 \, \mathrm{d}\omega \end{aligned}$$

Simplification for wiggler case

The angular and frequency spectrum of the radiation is then

$$\frac{\mathrm{d}^2 I}{\mathrm{d}\omega \mathrm{d}\Omega} = \frac{c\varepsilon_0}{\pi} \sum_{j=1}^{N_p} \left|\mathfrak{F}[\mathbf{u}_j(t)](\omega)\right|^2 = \sum_{j=1}^{N_p} \left.\frac{\mathrm{d}^2 I}{\mathrm{d}\omega \mathrm{d}\Omega}\right|_j$$

N_p ... number of turning points in electron sine-like trajectory

One peak of signal

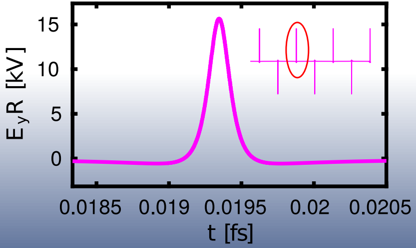

Total radiation summed

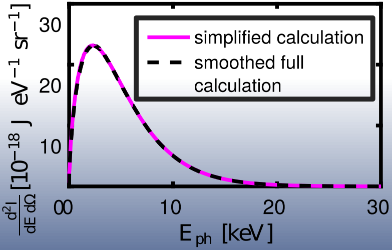

Simplification for wiggler case

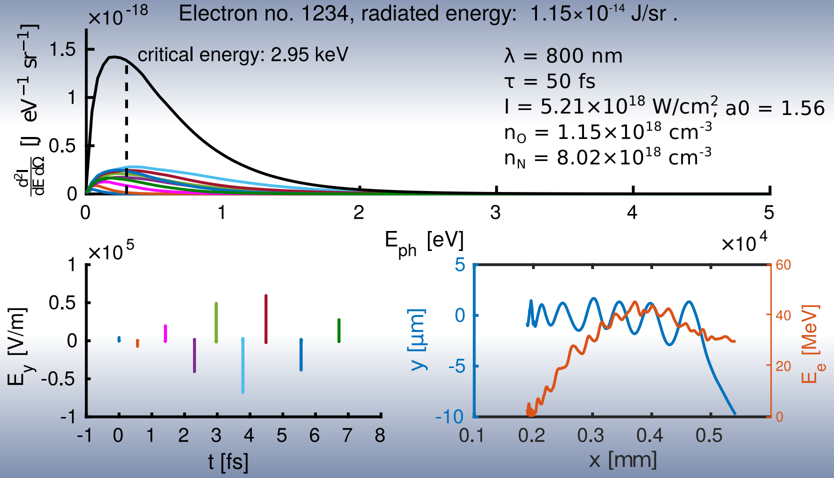

Simplification for wiggler case

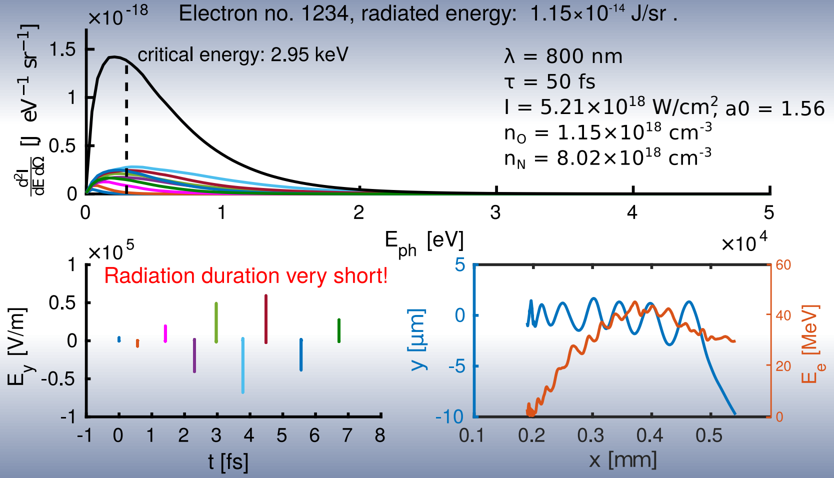

Radiation by electron bunch

Microbunching: free electron laser

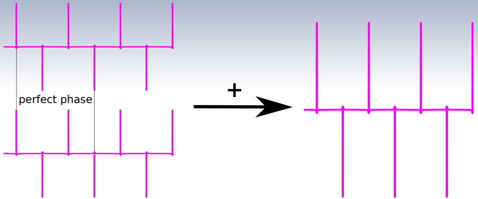

$$
\begin{aligned}
I &\sim (ER)^2 \\
E(t)R(t)|_{tot} &= N_e \, E(t)R(t)|_0 \\
I_{tot} &= N_e^2 I_0
\end{aligned}
$$

Radiation by electron bunch

Uniform distribution of electrons

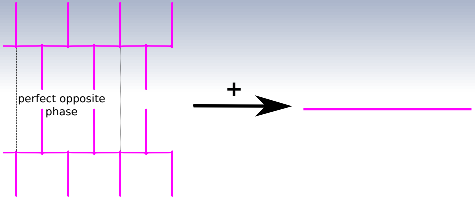

$$I \sim (ER)^2$$
$$ER|_{tot} = 0$$
$$I|_{tot} = 0$$

Radiation by electron bunch

Random distribution of electrons

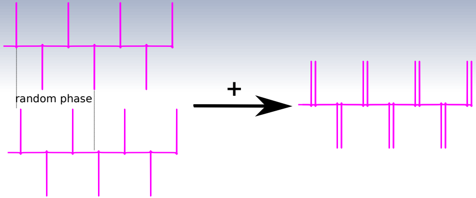

$$
\begin{aligned}
I &\sim (ER)^2 \\
E(t)R(t)|_{tot} &\neq N_e\, E(t)R(t)|_0 \\
I_{tot} &= N_e I_0
\end{aligned}
$$

Radiation by electron bunch

Random distribution of electrons

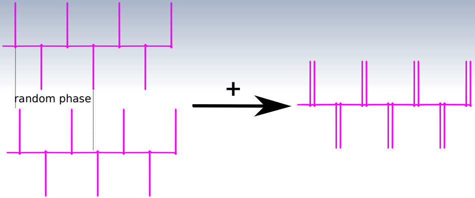

$$
\begin{aligned}
I &\sim (ER)^2 \\
E(t)R(t)|_{tot} &\neq N_e\, E(t)R(t)|_0 \\
I_{tot} &= N_e I_0
\end{aligned}
$$

Assumption of incoherence of electrons in the bunch

$$\frac{\mathrm{d}^2 I}{\mathrm{d}\omega \mathrm{d}\Omega} = \sum_{i=1}^{N_e} \frac{\mathrm{d}^2 I_i}{\mathrm{d}\omega \mathrm{d}\Omega} \approx N_e \left.\frac{\mathrm{d}^2 I}{\mathrm{d}\omega \mathrm{d}\Omega}\right|_{ave}$$

Contributions by single electrons may be summed up!

Spectrograms

When two assumptions are fulfilled

1. incoherent nature of electron bunch
2. wiggler regime of betatron oscillations,

temporal profile of radiation can be derived:

$$\frac{\mathrm{d}^2 I}{\mathrm{d}\omega \mathrm{d}\Omega} = \sum_{i=1}^{N_e} \sum_{j=1}^{N_{p,i}} \left. \frac{\mathrm{d}^2 I}{\mathrm{d}\omega \mathrm{d}\Omega} \right|_{ij} = \sum_{k=1}^{N_p} \left. \frac{\mathrm{d}^2 I}{\mathrm{d}\omega \mathrm{d}\Omega} \right|_{k}$$

$$\left. \frac{\mathrm{d}^2 I}{\mathrm{d}\omega \mathrm{d}\Omega} \right|_{t \in [\tau - \Delta t, \tau + \Delta t]} = \sum_{k | t_k \in [\tau - \Delta t, \tau + \Delta t]} \left. \frac{\mathrm{d}^2 I}{\mathrm{d}\omega \mathrm{d}\Omega} \right|_{k} \approx \frac{\mathrm{d}^3 I}{\mathrm{d}t \mathrm{d}\omega \mathrm{d}\Omega}$$

Duration of one peak is much shorter than considered resolution of spectrogram.

X-rays using 100 TW system

Laser system parameters

- energy in beam: 2.65 J
- pulse duration: 40 fs
- waist size: 9 µm
- $a_0 = 4$

Target parameters

- plasma density 1.5×10^{19} cm^{-3}
- linear density ramp 40 µm
- 2 mm of homogeneous plasma

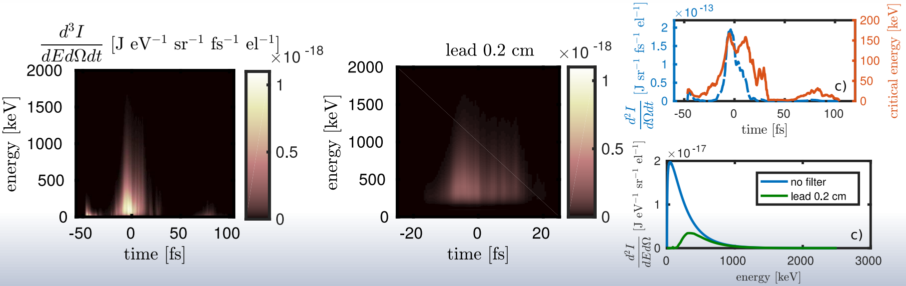

Continuous injection, electron energy up to 380 MeV.
Critical energy 127 keV, x-ray pulse length 13.7 fs.

Experiment at PALS [2]: Radiation estimation

Parameters

$\tau_L = 50$ fs, $E = 0.36$ J,
$n_e = 5 \times 10^{19}$ cm^{-3}

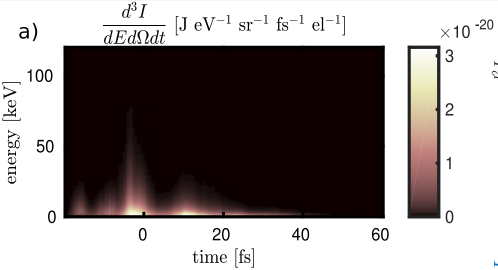

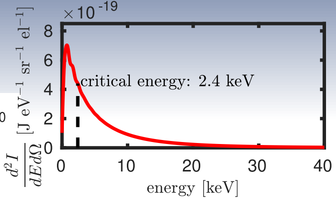

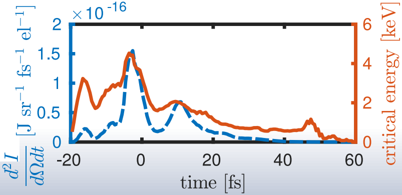

$E_c = 2.4$ keV, $\tau = 30$ fs

[2] Boháček, K.,. . . , Horný, V.,. . . (2018). *Stable electron beams from laser wakefield acceleration with few-terawatt driver using a supersonic air jet.* NIMA, 883, 24-28.

Novel crossed pulses optical scheme

Laser system parameters

- energy in beam: 2.65 J
- pulse duration: 40 fs
- waist size: 9 µm
- $a_0 = 4$

Target parameters

- plasma density 4.0×10^{18} cm^{-3}
- linear density ramp 40 µm
- 2 mm of homogeneous plasma

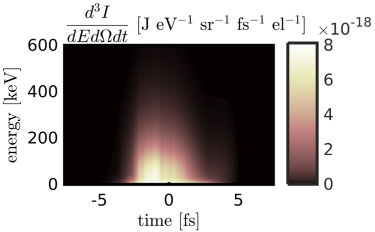

Critical energy 54 keV, x-ray pulse length 2.4 fs.

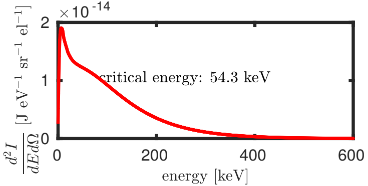

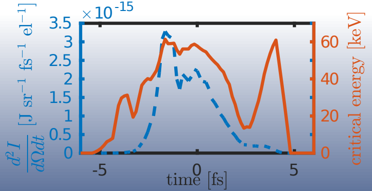

Conclusion

1. X-ray radiation features are determined by the quality of laser accelerated electron bunches.
2. Novel injection schemes can deliver high charge (tens of pC) and short length (fs) electron bunches.
   - orthogonally crossed pulses with parallel polarizations
   - injection by a preceding pulse
3. The method enabling calculation of the betatron radiation spectrogram was developed.
4. 2 fs long X-ray pulses can be generated. Such duration is shorter than fundamental physical processes such as chemical reactions, lattice vibrations etc.

Prospects for further work

- injection dynamics
- collection volume
- coherent radiation
- bubble dynamics
- shape of pulses
- tunability

Ponderomotive force

Comment

"... the terminology used is somehow vague in what is concerning the ponderomotive force and radiation force definition."

Response

- agreed, this paragraph should have been either omitted, or defined more accurately
- this term was introduced because it was used when discussing bubble formation and evolution
- it is not an important term for defended dissertation

Transverse wake wave breaking

Comment

"... when the author discusses the effects of 3-dimentional geometry on the electron injection he does not implement well known mechanism of transverse wake wave breaking."

Response

The following important reference is missing in my dissertation.
Bulanov, S. V., Pegoraro, F., Pukhov, A. M., and Sakharov, A. S. (1997). Transverse-wake wave breaking. *Physical Review Letters*, 78(22), 4205.

The effect of *transverse wake wave breaking* was discovered earlier than the *bubble regime*. Only bubble regime was discussed in defended dissertation.

Pellicle beamsplitter

Comment

"Author proposes to make a temporal splitting of a pulse by using a pellicle placed at a proper distance from a flat mirror. There are several methods to create multiple pulses, each of them having limitation due to complexity, stability or efficiency. This is why, in my opinion, more detail of the new scheme should have been presented in the thesis. More specifically, general flatness (not roughness) of a pellicle is not a stable parameter. So, what's about the focusing properties of the first pulse? How the author faces with multiple reflections? I strongly suggest the candidate to go in deeper detail with his scheme."

Double pulse generation

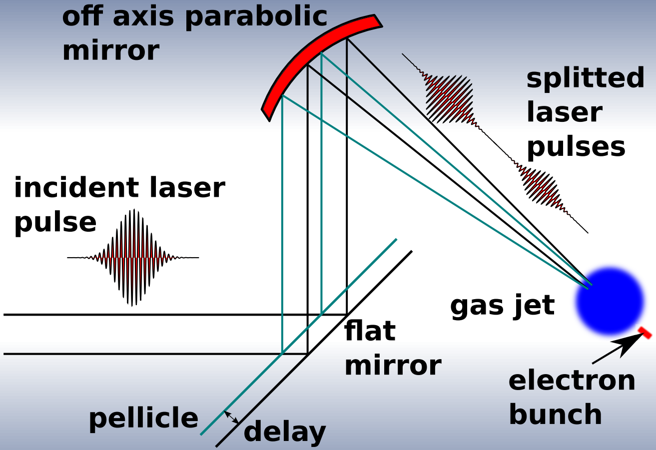

It is advisable to use the same focusing optics for both pulses.

Pellicle beamsplitter

Response

- pellicle beamsplitter: just the first idea
  - multiple reflections
  - unstable pellicle flatness
- **dazzler**: more sophisticated way
  - acousto-optics programmable dispersive filter[1]
  - about € 50 000
  - copy of pulses
  - interference of pulses ⇒ more pulses generated
- interferometry (delay line)
  - Michelson interferometer
  - Mach-Zender interferometer

[1] Tournois, P. (1997). Acousto-optic programmable dispersive filter for adaptive compensation of group delay time dispersion in laser systems. *Optics communications*, 140(4-6), 245-249.

Pellicle beamsplitter

Response

- pellicle beamsplitter: just the first idea
  - multiple reflections
  - unstable pellicle flatness
- **dazzler**: more sophisticated way
  - acousto-optics programmable dispersive filter[1]
  - about € 50 000
  - copy of pulses
  - interference of pulses ⇒ more pulses generated
- interferometry (delay line)
  - Michelson interferometer
  - Mach-Zender interferometer

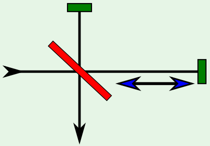

[1] Tournois, P. (1997). Acousto-optic programmable dispersive filter for adaptive compensation of group delay time dispersion in laser systems. *Optics communications*, 140(4-6), 245-249.

Pellicle beamsplitter

Response

- pellicle beamsplitter: just the first idea
  - multiple reflections
  - unstable pellicle flatness
- **dazzler**: more sophisticated way
  - acousto-optics programmable dispersive filter[1]
  - about € 50 000
  - copy of pulses
  - interference of pulses ⇒ more pulses generated
- interferometry (delay line)
  - Michelson interferometer
  - Mach-Zender interferometer

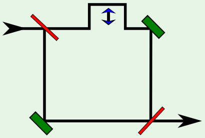

[1] Tournois, P. (1997). Acousto-optic programmable dispersive filter for adaptive compensation of group delay time dispersion in laser systems. *Optics communications*, 140(4-6), 245-249.

Beam quality limit

Comment

"Beam quality is nowadays a crucial parameter for application (including Thomson or FEL X-rays sources). The two collinear pulses scheme looks promising but simulations presented by the candidate reveal some limitation to beam quality, both on longitudinal and transverse directions. So, in the opinion of the candidate, which are the main physical (or numerical) processes that limit beam quality in this scheme? For instance it is known that most of the PIC codes (including EPOCH) induce a numerical growth of transverse emittance. Do different codes give rise to the same results?"

Growing emittance in simulations

Transverse emittance

$$\varepsilon_y = \sqrt{\langle y^2\rangle\langle p_y^2\rangle - \langle y p_y\rangle^2}/m_e c$$

remains constant during the acceleration (Liouville's theorem).

It grows with standard 2nd order Yee's scheme!

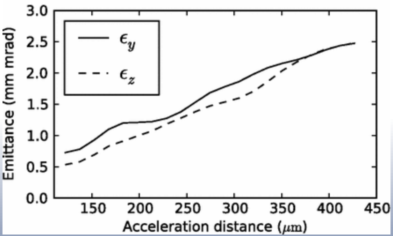

Figure taken from Lehe, R., Lifschitz, A., Thaury, C., Malka, V., and Davoine, X. (2013). Numerical growth of emittance in simulations of laser-wakefield acceleration. *Physical Review Special Topics-Accelerators and Beams*, 16(2), 021301.

Numerical Cherenkov radiation

Injection by a preceding pulse

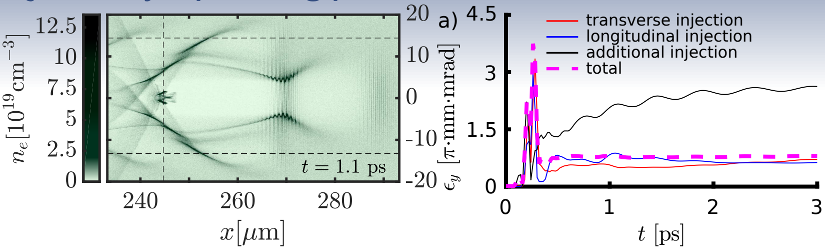

Figures from Horný, V., Mašlárová, D., Petržílka, V., Klimo, O., Kozlová, M., and Krůs, M. (2018). Optical injection dynamics in two laser wakefield acceleration configurations. *Plasma Physics and Controlled Fusion*, 60(6), 064009.

Emittance growth was mitigated introducing 6$^{\mathrm{th}}$ order scheme. Even though the improved Lehe's scheme was implemented into EPOCH recently, it does not work well yet!

Numerical Cherenkov radiation

Injection by a preceding pulse

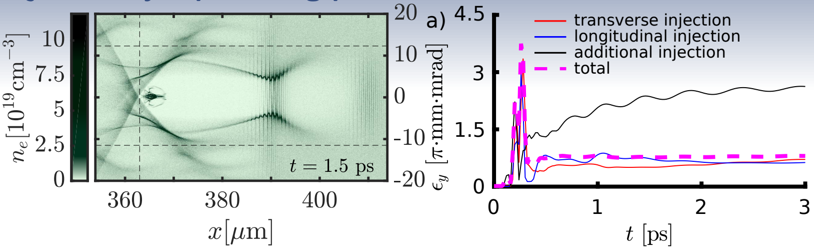

Figures from Horný, V., Mašlárová, D., Petržílka, V., Klimo, O., Kozlová, M., and Krůs, M. (2018). Optical injection dynamics in two laser wakefield acceleration configurations. *Plasma Physics and Controlled Fusion*, 60(6), 064009.

Emittance growth was mitigated introducing 6th order scheme. Even though the improved Lehe's scheme was implemented into EPOCH recently, it does not work well yet!

Limitation of the beam quality

Considerable influences

Among practical issues such as laser beam/system or gas jet quality:

1. Collection volume size of trapped electrons
2. Injection dynamics
3. *Off-axis injection*: large initial transverse momentum
4. Beam-loading effect
5. Bubble dynamics during the acceleration phase

Suggestion for further research

1. Tailored density profile
   - transverse: wave guide
   - longitudinal: bubble dynamics compensation, phase space rotation
2. Adjustable laser pulse temporal and spacial profiles

Betatron X-ray pulse duration

Comment

"Author claims that the X-ray burst generated by betatron oscillation in the case of the optical injection schemes is much shorter than we can infer by the standard formula L/c. This is a very interesting result that definitely deserves to be understood in deeper detail. Which are the reasons of such a discrepancy? What are the key parameters that trigger it? Can we infer some scaling laws for that?"

Response

- interpretation of a bunch length
- non-uniform distribution of electrons in the bunch
- short duration of radiation of a single electron